Meta and para substitution effects on the electronic state energies and ring-expansion reactivities of phenylnitrenes

ARTICLE *in* INTERNATIONAL JOURNAL OF QUANTUM CHEMISTRY · NOVEMBER 2001

Impact Factor: 1.43 · DOI: 10.1002/qua.1518

3 AUTHORS, INCLUDING:

Christopher J Cramer
University of Minnesota Twin Cities
531 PUBLICATIONS **23,105** CITATIONS

meta and *para* Substitution Effects on the Electronic State Energies and Ring-Expansion Reactivities of Phenylnitrenes

WILLIAM T. G. JOHNSON, MICHAEL B. SULLIVAN, CHRISTOPHER J. CRAMER

Department of Chemistry and Supercomputer Institute, University of Minnesota, 207 Pleasant St. SE, Minneapolis, Minnesota 55455-0431

Received 25 February 2001; revised 26 March 2001; accepted 26 March 2001

ABSTRACT: The electronic structures of the triplet ground states and first three excited singlet states for phenylnitrene, 14 *meta*-, and 17 *para*-substituted congeners have been characterized using density functional theory and multireference second-order perturbation theory (CASPT2). Ring expansion pathways to form didehydroazepines have activation enthalpies of about 9 kcal · mol^{-1} and are fairly insensitive to substitution—in the case of the strongest *para* donor, MeNH–, this barrier increases to about 13 kcal · mol^{-1}. The trends in state energies as a function of substitution are rationalized using a (2,2) configuration interaction theory and qualitative molecular orbital theory. Analysis of spin-orbit coupling in the nitrenes using the same model in conjunction with explicit calculation of spin-orbit coupling matrix elements rationalizes why electron donating substituents increase rates of intersystem crossing. Int J Quantum Chem 85: 492–508, 2001

Key words: photoaffinity labels; ring expansion; photochemistry; nitrene; didehydroazepine; configuration interaction; excited states; density functional theory

Correspondence to: C. J. Cramer; e-mail: cramer@chem.umn.edu.

Contract grant sponsors: National Science Foundation; Alfred P. Sloan and John Simon Guggenheim Foundations; Spanish Ministry of Education and Culture; and Fundación BBV.

This article includes supplementary material available at http://www.interscience.wiley.com/jpages/0020-7608/suppmat/85_4-5/v85_4-5.html

Introduction

Phenylnitrenes [1–3] are reactive intermediates readily generated from photolysis of antecedent phenyl azides. These hypovalent species have a number of low-lying electronic states. Experiment [1, 4–9] and theory [8, 10–15] have established that the ground state of phenylnitrene is a triplet (T0), the first excited singlet state (S1) has open-shell character similar to the triplet, and there are two singlets having closed-shell character (S2 and S3) lying somewhat higher in energy. Illustrations of the dominant electronic configurations contributing to these different states are given in Figure 1. In substituted phenylnitrenes, it is clear that the triplet state continues to be the ground state, but the character of the first three singlet states has not been exhaustively explored in most instances [12].

Because most biomolecules are transparent to the wavelength required for the photolysis of a phenyl azide, various phenylnitrenes have proven useful as photoaffinity labels [16–28]. To act as a label, the nitrene must covalently attach (by bond insertion) to the active site of the biomolecule with which it is complexed. The utility of phenylnitrenes in this reaction, however, can be mitigated by the presence of unimolecular reactions that proceed at rates higher than the desired bimolecular reaction. Two such unimolecular processes that have been reasonably well characterized are intersystem crossing (ISC) from the reactive singlet state to the ground-state triplet, and ring expansion of the singlet to produce a didehydroazepine. Neither the triplet nor the didehydroazepine is particularly useful as a photoaffinity label: the triplet is reactive only as a hydrogen-atom abstracting agent, and while the didehydroazepine can react with nucleophiles in a fashion that results in covalent attachment, if the active site does not contain any nucleophiles, then migration of the heterocycle to some other region of the biomolecule prior to reaction can result in misinformation about the active site. The relative rates of the desired nitrene bond insertion versus these unproductive reactions have been shown to be sensitive to substituents on the aromatic ring in several instances (Fig. 2). Another competing reaction that can occur in a suitably acidic aqueous medium is protonation to the corresponding nitrenium ion [28–34], but that chemistry will not be the subject of further investigation here (the nitrenium ion is also hypovalent and can react via bond insertion, but formation of nitrenium ions is unlikely in any but the most polar of active sites).

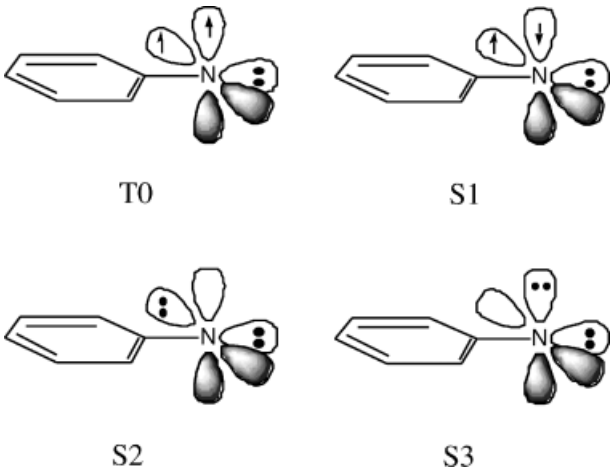

FIGURE 1. Dominant configurations contributing to the different electronic states of phenylnitrene. For properly antisymmetric wave functions, see Eqs. (2–5) and accompanying discussion.

In the absence of heavy atoms, ISC is often sufficiently slow so that the main competing pathway is ring expansion. This expansion, illustrated in Figure 3, may formally be viewed as a Wagner–Meerwein shift of carbon to the electron deficient nitrogen [35]. The product didehydroazepine thus correlates in a diabatic sense with the third excited singlet state. As such, it has been proposed that electron donating substituents, which would be expected to raise the energy of this state since it is already π-rich, will similarly increase the energy of the ring-expansion transition state(s), that must involve some mixing of the character of this singlet with those of the lower lying ones [2, 12].

However, the microscopic pathway for ring expansion does not really much resemble a Wagner–Meerwein shift. As shown in Figure 4, theory indicates that it begins with nitrene **1** closing back on the π cloud of the aromatic ring via transition state (TS) structure **2** to form strained bicycle **3**, which passes through TS **4** via a thermally allowed disrotatory pericyclic ring opening of the cyclohexadiene to form didehydroazepine **5** [3, 14, 36, 37]. Based on calculations for *ortho* fluoro- and -methyl-substituted **1**, and analysis of experimental results that show doubly *ortho*-substituted nitrenes to be most resistant to ring expansion [2, 38] and *para*-substituted nitrenes to be quite susceptible to such expansion over a range of π-electron-withdrawing to weakly donating groups [26, 37], Borden and

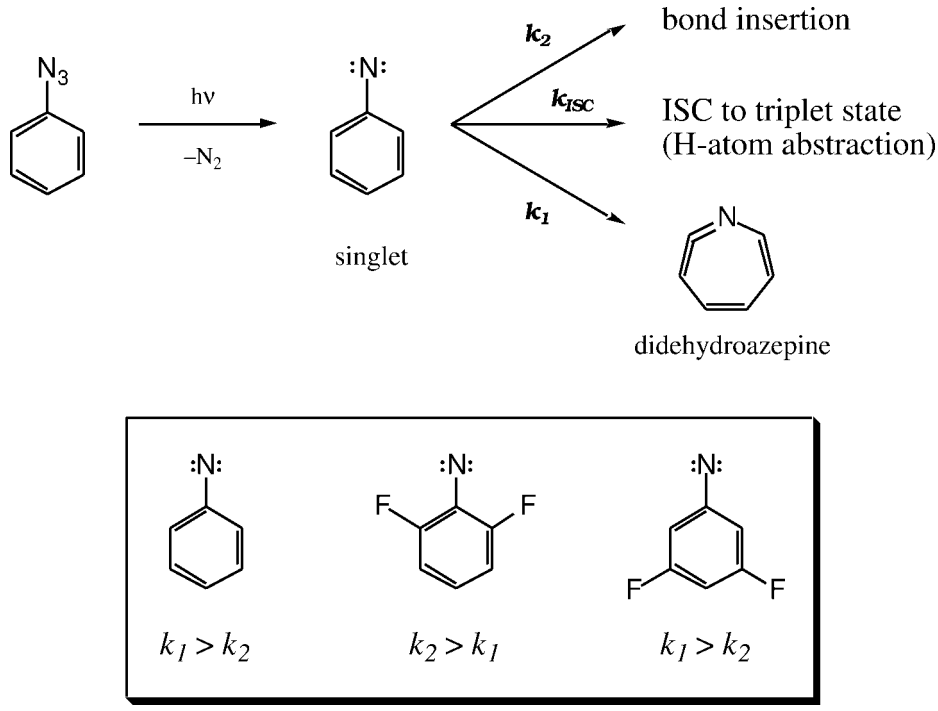

FIGURE 2. Photochemical activation of phenyl azide and reactive pathways for the intermediate nitrene. Sensitivity of partitioning between reactive channels to aromatic substitution is illustrated with selected experimentally characterized examples [20].

co-workers have emphasized a steric basis for the inhibition of ring expansion in phenylnitrenes [3, 14, 36, 37].

A few questions remain from these earlier studies. The computational results of Karney and Borden [14] indicate the ring expansion barrier in phenylnitrene doubly *ortho* substituted with fluorine to be slightly larger than for double substitution with methyl. Since this ordering is *not* what one would expect on a steric basis alone, it suggests that some electronic difference between fluorine and methyl may also contribute. Moreover, the experimental results for systems *para*-substituted with moderate to strong π donors are clouded because the rates of ISC become too large in these systems to permit any measurement of the cyclization barrier. Why there *is* a substitution effect on the rate of ISC has not been explored at all.

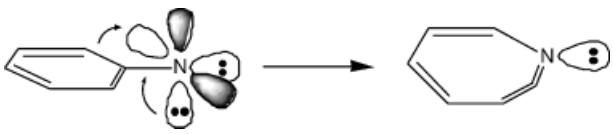

FIGURE 3. Nitrene ring expansion, rationalized as a Wagner–Meerwein shift, diabatically correlates the didehydroazepine ground state with the S3 singlet state.

In this work, in order to probe exclusively the electronic effect of substitution, we compute the triplet and 3 singlet state energies for phenylnitrene and 31 singly substituted derivatives (17 *para* and 14 *meta*). For four of these species, spanning the range of electron-withdrawing/donating character of the substituents as judged by their Hammett σ constants [39, 40], we characterize the ring expansion pathway. Finally, we compute spin-orbit coupling constants in order to better understand the factors affecting rates of ISC in the different substituted systems. All calculations are carried out at both the density functional (DFT) and multireference second-order perturbation (CASPT2) levels of theory. The following section describes the methodology, with special attention paid to the possible limitations of DFT for certain of the singlet states. We then detail the results of the calculations, and finally discuss the results, both in the context of previous work and within the framework of a (2,2) configuration interaction (CI) description [41 – 43] of the nitrene.

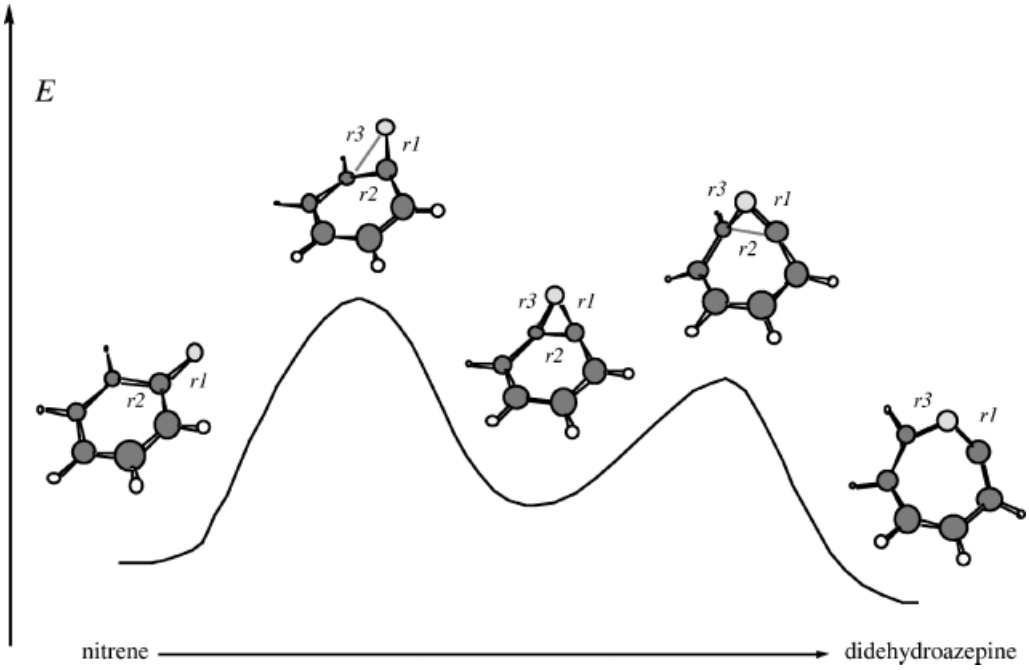

FIGURE 4. Reaction coordinate for ring expansion converting arylnitrene to didehydroazepine with computed geometries of stationary points represented. Key bonds whose lengths can be found in Table II are labeled.

Computational Methodology

MULTIREFERENCE

All structures were fully optimized at the multiconfiguration self-consistent field level using a complete-active-space approach (CASSCF) [44]. The basis set employed for all atoms other than bromine and iodine was the correlation-consistent polarized valence-double-ζ basis set of Dunning (cc-pVDZ) [45]. For multireference calculations involving bromine [46] or iodine [47], the Cowan–Griffin ab initio model potential with a relativistic effective core potential was used. The valence basis for bromine was contracted into three s functions, four p functions, and two d functions. The valence basis set for iodine was contracted into three s functions, four p functions, and three d functions. Analytic computation of vibrational frequencies was undertaken for all structures along ring expansion reaction coordinates to verify their nature as stationary points and to compute partition functions under the usual ideal-gas, rigid-rotor, harmonic-oscillator assumptions [48].

For the nitrenes, the CAS was formed from the 6 π orbitals of the aromatic ring and the 2 nitrene nitrogen p orbitals; this active space was occupied by 8 electrons. This (8 $\times$ 8) space was reduced to the 6 electrons in the 6 π orbitals for the analogous benzenes employed in isodesmic reactions described further below. Along ring-expansion reaction paths, active spaces were chosen so as to maximize diabatic correspondence with the nitrene [49]. For transition states **2** and **4**, the 6 π electrons and 6 π orbitals of the aromatic ring were combined with the two electrons and orbitals of the forming or breaking bond to define the (8 $\times$ 8) active space. For minimum **3**, the 2 electrons and orbitals of the bicyclic bond joining the two rings were combined with the 6 electrons and orbitals of the π bonds to form a corresponding active space, while for minimum **5** the 8 electrons and orbitals are all associated with π bonding.

To account for dynamical electron correlation, and to make up for a certain degree of arbitrariness in assigning the active space for **3**, CASPT2 calculations were carried out for all CAS-optimized geometries using the CASSCF wave functions for reference [50–52]. Some caution must be applied in interpreting the CASPT2 results since this level of theory tends to suffer from a systematic error proportional to the number of unpaired electrons [52, 53].

Spin-orbit coupling constants (SOCs) were calculated using the full Pauli–Breit Hamiltonian. These

calculation used the optimized CASSCF(8,8)/cc-pVDZ geometries for the lowest singlet state.

CAS geometry optimizations were accomplished using primarily the MOLCAS [54], but also the Gaussian 98 [55] and MOLPRO [56] suites of electronic structure programs. Calculations of SOCs was accomplished using GAMESS [57].

DENSITY FUNCTIONAL THEORY

The gradient-corrected exchange functional of Becke [58] was combined with the gradient-corrected correlation functional of Perdew and Wang [59] (BPW91) for all DFT calculations. Because the PW91 functional led to instability in the SCF equations early in the ring-expansion reaction coordinate, the gradient-corrected functional of Lee, Yang, and Parr [60] (BLYP) was also examined in this context. Geometries were fully optimized for all species, and analytic computation of vibrational frequencies was carried out to confirm the nature of stationary points and to compute partition functions along ring expansion reaction coordinates. The cc-pVDZ basis set was employed for all atoms other than bromine and iodine, for which the LANL2DZ+ effective-core-potential basis set [61–63] was used.

There are important issues associated with a DFT description for some of the nitrene electronic states. The Hohenberg–Kohn theorem [64], as later generalized making use of group theory by Gunarsson and Lundqvist [65], proves the existence of a functional of the density for computing the energy for the (nondegenerate) systems of lowest energy with wave function spatial symmetries belonging to each irreducible representation (irrep) of the molecular point group. In the case of the nitrenes, S2 and S3 always belong to the totally symmetric irrep since they are closed-shell singlets. Unless the nitrene has no symmetry, T0 does *not* belong to the totally symmetric irrep, so DFT may be reasonably expected to be robust for computing the properties of T0 and S2. In the absence of symmetry, there is no formal guarantee that this should be the case (since then *all* electronic states belong to the same irrep), but in practice singlet-triplet splittings between triplets and closed-shell singlets seem to be robustly calculated by DFT even in the absence of different electronic state symmetries for a variety of systems [66–68].

In the case of S3, we have been successful in every case but *m*-nitro in converging the DFT SCF equations for orbital occupations corresponding to those that would be expected to be occupied in a Slater determinant representation of the configuration state function corresponding to S3. However, even in Hartree–Fock theory, there is no reason to expect such a wave function to be particularly good, since it does not represent a variational minimum. Even more so, in the DFT formalism, caution should be exercised in the interpretation of results for this state. Although time-dependent DFT methods might in principle be applied to the description of this excited state [69], in practice we found available implementations of such models to be too unstable to be useful.

As for S1, it always has the same state symmetry as T0 since the only difference between the two states is spin-coupling. Moreover, S1 is an intrinsically two-determinant wave function, and insofar as DFT within the Kohn–Sham implementation is an intrinsically single-determinant formalism, it is not obvious how to go about representing this state. In this work, we have employed unrestricted DFT with an equal number of α and β electrons and found broken-symmetry solutions. There is an ongoing debate about the degree to which such a formalism describes a pure singlet as opposed to a mixture of spin states [53, 68, 70–77]. In the nitrene case, if a Slater determinant is formed from the occupied DFT orbitals, it is found to have an expectation value for the total spin operator (S^2) of exactly 1.0 in every instance. Ziegler et al. [70] were the first to suggest that DFT in this instance should be regarded as describing a 50:50 mixture of singlet and triplet spin states, and they proposed a sum method whereby the energy of the pure singlet state could be determined. We have followed that prescription here and, as noted below, it gives reasonable results in comparison with CASPT2. However, it must then be borne in mind that geometries for S1, and thermochemical quantities derived from analytic vibrational frequencies used for the ring expansion reaction coordinate, are poisoned by a 50% contribution from T0 (unless one were to carry out optimizations and frequency analyses by hand using the sum method energies—analytic derivatives are not available).

With respect to the importance of broken-symmetry DFT solutions along the singlet ring-expansion reaction coordinates, all restricted calculations of structures **3**, **4**, and **5** were found to be stable to symmetry breaking. For TS structures **2**, in the case of R = NHMe, the restricted solution was stable, but this was *not* the case for the other substituents examined. Unfortunately, convergence of the wave function could not be achieved in those

instances with an unrestricted formalism in spite of considerable efforts. Insofar as the situation with one substituent indicates a restricted solution to be stable, we do not expect there to be a large error in using that solution for the other cases, but it should be born in mind that the energy in those instances is probably slightly overestimated (i.e., the corresponding barrier is predicted to be a bit too high).

All DFT calculations were carried out with Gaussian 98 [55].

Results

RING EXPANSION REACTION COORDINATES

Optimized structures for most stationary points **1–5** were located at the BPW91, BLYP, and CAS levels of theory for R = NHMe, H, F, and NO_2. These 4 choices span the range from highly electron-donating (NHMe, Hammett σ value of -0.46) to highly electron-withdrawing (NO_2, Hammett σ value of 0.81), include the parent unsubstituted system, and F, which has been studied as an *ortho* substituent by Karney and Borden [14] and as a *para* substituent by Gritsan et al. [38] for that portion of the reaction coordinate following closure to the benzazirine.

Use of the PW91 correlation functional, motivated in part to facilitate comparison to prior results [12], led to considerable instability early in the ring expansion reaction coordinate, and locating TS structures **2** was particularly problematic. To examine the extent to which this was influenced by choice of functional, we also surveyed the BLYP level of theory. This functional combination was considerably more robust, although as noted in the Methods section, restricted DFT determinants for structures **2** were unstable to unrestricted symmetry breaking for all cases but R = NHMe, and the unrestricted SCF could not be coaxed to convergence. As indicated in Table I, which lists the 298 K enthalpies of the stationary points relative to **1** as computed at the three levels of theory, the BLYP and CASPT2 relative energies are in reasonably good agreement, while the BPW91 relative energies are systematically too high by 2–4 kcal · mol^{-1} for **3–5**, and as much as 8 kcal · mol^{-1} for the unstable restricted SCF energies for **2**. This systematic error presumably reflects an overstabilization of the S1 reference state by the BPW91 functional (vide infra). As we are interested in more quantitative results for the ring-expansion reaction coordinates, we carry out our analysis for this subject using only the CASPT2 and BLYP data (by contrast, to understand the nature of substitution effects on the nitrene state energies, qualitative accuracy is entirely acceptable, and BPW91 is deemed to be adequately representative as a functional as described in more detail below). Table II provides interatomic distances for the forming and breaking bonds, as labeled in Figure 4, for the BLYP and CAS stationary points along the reaction coordinates. We note that the energies of **4** and **5** relative to **3** for *p*-fluorophenylnitrene as computed at the CASPT2/cc-pVDZ//CAS(8,8)/6-31G* level by Gritsan et al. [38] agree to within 0.3 kcal/mol with our CASPT2 results in Table I (such agreement is to be expected insofar as the only difference is the basis set used for geometry optimization at the CAS level).

TABLE I

DFT and CASPT2 enthalpies (H_{298}, kcal · mol^{-1}) of stationary points 2–5 relative to 1 for different *para* substituents R.

R	Level	2	3	4	5
NHMe	BPW91	16.4	11.7	15.0	6.0
	BLYP	11.6	9.7	12.5	0.8
	CASPT2	12.3	8.5	13.3	1.7
H	BPW91	19.4[a]	5.0	7.3	1.4
	BLYP	11.2[a]	2.5	4.1	−4.4
	CASPT2	8.5	2.7	5.8	−1.9
F	BPW91	[b]	6.0	9.2	2.2
	BLYP	10.4[a]	3.5	5.9	−3.8
	CASPT2	8.9	3.0	7.3	−1.6
NO_2	BPW91	18.5[a]	4.6	5.7	1.1
	BLYP	11.1[a]	2.6	3.0	−4.3
	CASPT2	9.5	3.7	4.8	−0.7

[a] Restricted SCF solutions were unstable relative to unrestricted solutions; however, the latter could not be converged, and restricted values are listed.
[b] Neither a restricted nor an unrestricted SCF could be converged.

ELECTRONIC STATE ENERGIES

Table III lists the electronic energies of the three singlet states S1, S2, and S3 relative to the triplet as computed at the CASPT2 and BPW91 levels of theory for 32 nitrenes studied here. The T0 state was indeed the ground state in every case. The S1 energies at the BPW91 level have been computed using the sum method of Ziegler et al. [70, 72]. That is, the

TABLE II
Selected heavy-atom bond distances (Å) in structures 1–5.[a]

Structure	Bond	Level	NHMe	H	F	NO_2
1	*r*1	CAS	1.278	1.277	1.278	1.276
		BLYP	1.313	1.316	1.316	1.308
	*r*2	CAS	1.471	1.474	1.474	1.475
		BLYP	1.463	1.463	1.464	1.461
2	*r*1	CAS	1.261	1.261	1.262	1.260
		BLYP	1.275	1.286	1.281	1.280
	*r*2	CAS	1.455	1.458	1.457	1.462
		BLYP	1.482	1.488	1.487	1.494
	*r*3	CAS	2.060	2.066	2.067	2.073
		BLYP	1.969	2.276	2.189	2.274
3	*r*1	CAS	1.261	1.260	1.261	1.259
		BLYP	1.281	1.277	1.279	1.271
	*r*2	CAS	1.437	1.442	1.440	1.443
		BLYP	1.503	1.520	1.510	1.540
	*r*3	CAS	1.637	1.631	1.633	1.627
		BLYP	1.619	1.597	1.599	1.595
4	*r*1	CAS	1.253	1.251	1.253	1.245
		BLYP	1.267	1.262	1.264	1.258
	*r*2	CAS	1.774	1.774	1.777	1.765
		BLYP	1.755	1.754	1.764	1.735
	*r*3	CAS	1.465	1.469	1.466	1.473
		BLYP	1.517	1.526	1.518	1.537
5	*r*1	CAS	1.258	1.257	1.255	1.253
		BLYP	1.272	1.265	1.267	1.255
	*r*3	CAS	1.417	1.420	1.418	1.422
		BLYP	1.426	1.440	1.431	1.454

[a] See Figure 4 for bond labeling.

energy is computed as

$$E(\mathrm{S1}) = 2 \times E(\mathrm{50{:}50}) - E(\mathrm{T0}) \qquad (1)$$

where E(50:50) is the energy of the broken-symmetry unrestricted DFT wave function having an expectation value of 1 for the S^2 operator applied to a Slater determinant formed from the DFT orbitals (i.e., the exact wave function for the noninteracting Kohn–Sham reference system), and E(T0) is the energy of the triplet. The geometry for all energy calculations is that optimized for the 50:50 state (which is a potential drawback of the sum method). Irrespective of method, the T0–S1 splitting is effectively a constant independent of substitution.

We are interested primarily in trends in state energies as a function of substitution, and not absolute accuracy. With such a goal, the polarized double-ζ basis sets used here can be considered to be adequate. Some assessment of the absolute accuracy can be had by comparison to experiment and prior calculations at the same levels of theory with larger basis sets, however. For the parent, unsubstituted system, the experimental energies of the S1 and S2 states relative to T0 are 18 [5] and 30 [78] kcal·mol^{-1}, respectively. As listed in Table III, the CASPT2/cc-pVDZ predictions are 19.3 and 37.4 kcal · mol^{-1}, respectively, and the BPW91/cc-pVDZ predictions are 14.3 and 33.9 kcal · mol^{-1}, respectively (note, as mentioned above, the overstabilization of the S1 state). While basis set size would be expected to have minimal impact on the T0–S1 splitting, since the two states have formally identical spatial configurations, predictions for the T0–S2 splitting using the same geometries but the cc-pVTZ basis set are 34.8 and 29.5 kcal · mol^{-1} at the CASPT2 and BPW91 levels, respectively [12]. For the T0–S1 splitting, then, CASPT2 is more quantitatively accurate; the DFT sum method overstabilizes the S1 state and thus underestimates the splitting by 4 kcal · mol^{-1}. For the T0–S2 splitting, at each level of theory the use of a double-ζ basis set contributes about 3 kcal · mol^{-1} of error in overestimating the gap. Of the two theories, the DFT level is the more accurate, being essentially quantitative with the triple-ζ basis set. The moderate overestimation of the T0–S2 splitting at the CASPT2 level even with the cc-pVTZ basis set is consistent with the usual behavior of this level of theory when comparing species having different numbers of unpaired electrons [52, 53]. Accurate gas-phase state energies are not available for other phenylnitrenes. Similarly, no experimental value exists for the T0–S3 splitting in the parent system, although the basis set size effects are about the same as for the T0–S2 analog [12].

Figures 5 and 6 represent the state energies from the two levels of theory graphically as a function of the Hammett σ parameter for the *meta* and *para* substituents. The parent nitrene is assigned a σ value of zero per the usual convention. At the CASPT2 level of theory, the illustrated configurations of Figure 1 are fairly good descriptions for all states across the entire span of substituents. At the BPW91 level, on the other hand, although symmetry restrictions permit these configurations to be enforced rigorously, the S2 and S3 state energies begin to intermingle at high positive values of σ (if we continue to apply the labels based on configuration instead of based on energetic ordering). As described in further detail below, this is likely to be an artifact of the DFT methodology.

TABLE III

Hammett σ values and CASPT2 and BPW91 singlet energies (kcal · mol^{-1}) relative to T0 for R-substituted phenylnitrenes.

		S_1		S_2		S_3	
R	σ	CASPT2	BPW91	CASPT2	BPW91	CASPT2	BPW91
p-$NHCH_3$	−0.46	16.7	12.2	30.4	23.3	63.7	53.9
p-OH	−0.38	18.3	13.4	34.5	27.6	61.2	49.9
p-$N(CH_3)_2$	−0.32	16.3	12.2	30.5	24.4	63.2	52.4
p-NH_2	−0.30	17.1	12.5	31.2	23.9	63.5	53.4
p-CH_3	−0.14	18.8	13.8	36.9	32.2	58.6	44.5
p-OCH_3	−0.12	18.3	13.3	34.5	27.7	65.2	49.4
m-$N(CH_3)_2$	−0.10	19.3	14.1	36.7	32.7	57.4	43.0
m-$NHCH_3$	−0.10	19.6	14.3	36.8	33.1	57.0	42.8
m-NH_2	−0.09	19.2	14.1	37.1	33.3	57.2	43.2
m-CH_3	−0.06	19.5	14.3	37.3	33.6	57.6	43.1
H	0.00	19.3	14.3	37.4	33.9	57.8	43.0
m-OCH_3	0.10	20.0	14.7	37.4	33.9	57.1	43.1
m-OH	0.13	19.6	14.5	37.6	34.3	57.0	43.1
p-F	0.15	19.1	14.1	36.3	30.8	59.5	47.1
p-Cl	0.24	18.4	13.7	37.3	32.6	58.2	45.1
p-Br	0.26	18.4	13.8	37.5	33.0	57.9	44.5
p-I	0.28	18.2	13.7	37.7	33.1	57.4	43.7
m-F	0.34	19.4	14.4	37.9	34.3	57.5	43.9
m-I	0.34	19.3	14.2	37.6	32.2	57.2	41.8
m-$COCH_3$	0.36	19.8	14.7	37.7	35.1	57.1	39.2
m-Cl	0.37	19.4	14.3	37.8	[a]	57.5	43.3
m-Br	0.37	19.3	14.3	37.7	33.0	57.3	42.8
p-CO_2H	0.44	18.0	15.4	38.7	38.1	55.9	38.3
p-CO_2CH_3	0.44	18.0	13.4	38.6	36.7	56.0	37.7
m-CF_3	0.46	19.8	14.7	37.8	[a]	57.4	42.7
p-$COCH_3$	0.47	17.5	13.0	38.7	37.1	56.1	33.9
p-CHO	0.47	17.2	12.9	38.9	37.9	56.0	36.1
p-CF_3	0.53	19.1	14.2	38.3	40.7	62.8	36.1
m-CN	0.62	19.7	14.7	37.9	35.1	57.3	42.7
p-CN	0.70	17.5	13.2	39.5	37.0	56.7	40.6
m-NO_2	0.71	19.7	14.7	38.0	[a]	57.4	[a]
p-NO_2	0.81	18.1	13.5	38.8	38.3	55.5	34.1

[a] SCF convergence for this state was not achieved.

SPIN-ORBIT COUPLING

Table IV provides spin-orbit couplings between T0 and the different singlet states as computed at the CAS(8,8) level of theory using the full Pauli–Breit Hamiltonian. Within the C_{2v} point group, SOCs between T0 and S1 must be zero by symmetry, and actual calculation bears this out. In the case of R = NHMe, the lower symmetry in principle allows a nonzero SOC, but the value remains zero to within 0.1 cm^{-1}.

SOCs between T0 and S2 and T0 and S3 are allowed by symmetry, and calculation finds them to be on the order of 15 for the former state and 40 for the latter. The trend for SOC between T0 and S2 is that it increases with decreasing σ by a moderate margin, while the trend for SOC between T0 and S3 is that it decreases with decreasing σ by a very small amount.

Discussion

RING EXPANSION REACTION COORDINATES

Although significant differences between the BLYP and CAS geometries are manifest in several

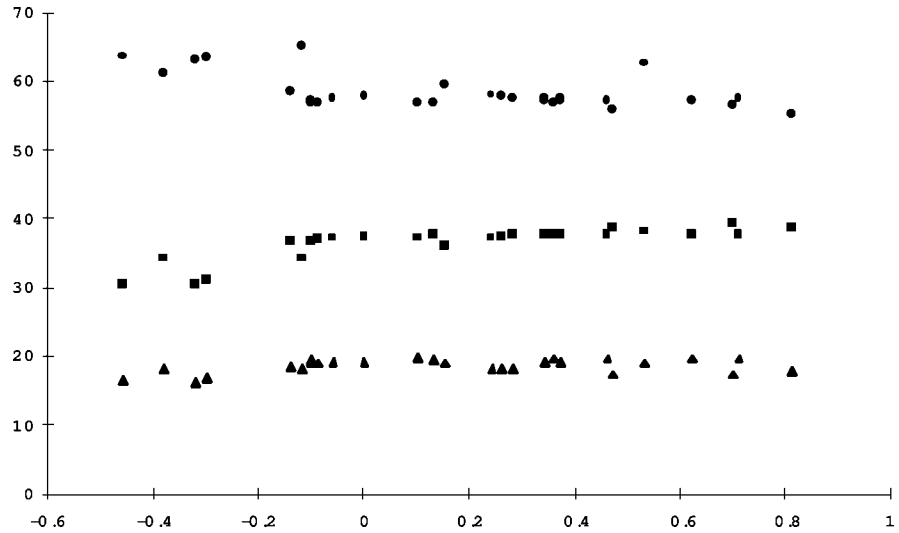

FIGURE 5. CASPT2 singlet state energies (kcal · mol^{-1}, S1 = triangles, S2 = squares, S3 = circles) relative to T0 for *meta* and *para* substituted phenylnitrenes as a function of substituent Hammett σ value.

instances (Table II), this derives at least in part from the very flat nature of the potential energy in various regions of the reaction coordinate. In such regions, large geometric distortions can occur with little energetic cost, and the exact position of a stationary point is, to some extent, arbitrary. Thus, in spite of somewhat different geometries, the predicted energies of the various stationary points **2**–**5** are in remarkable agreement in almost every case. Moreover, the agreement would presumably only be improved if convergence of the unrestricted DFT SCF for **2** could be accomplished for the H-, F-, and NO_2-substituted cases (where a restricted → unrestricted instability was noted) since this would presumably slightly lower the DFT energies and bring them more into line with those from CASPT2. We infer that the energy lowering would indeed be no more than the existing difference with CASPT2 because the restricted → unrestricted instability is absent in the NHMe-substituted case.

Insofar as both levels of theory give reasonably good agreement for the relative energetics, we conclude with some confidence that the trends as a function of substituent can be regarded as mean-

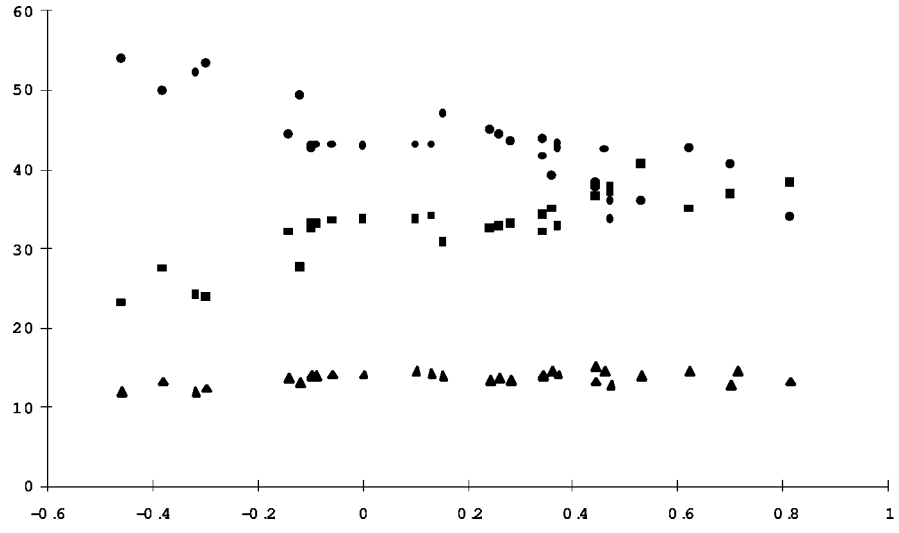

FIGURE 6. BPW91 singlet state energies (kcal · mol^{-1}, S1 = triangles, S2 = squares, S3 = circles) relative to T0 for *meta* and *para* substituted phenylnitrenes as a function of substituent Hammett σ value.

TABLE IV

Spin-orbit coupling constants for the first three singlet states of four substituted phenylnitrenes (cm^{-1}).

State	R = NO_2	R = F	R = H	R = NHMe
S_1	0.0	0.0	0.0	0.0
S_2	11.9	16.6	15.5	18.8
S_3	44.3	43.5	43.5	41.8

ingful. Chief among these is the observation that the reaction coordinates for the H-, F-, and NO_2-substituted cases are essentially indistinguishable, all being weakly exothermic with formation of **3** as the rate-determining step. By contrast, for the NHMe-substituted case, ring expansion is predicted to be weakly *endo*thermic, and it is the electrocyclic *opening* of **3** that is predicted to be rate-determining. The overall difference in enthalpy of reaction is about 3 to 5 kcal · mol^{-1}. We rationalize this modest substituent effect on the reaction coordinate as deriving in part from a favorable interaction between an electron withdrawing group and the didehydroazepine as indicated by the following resonance using the nitro group as an example:

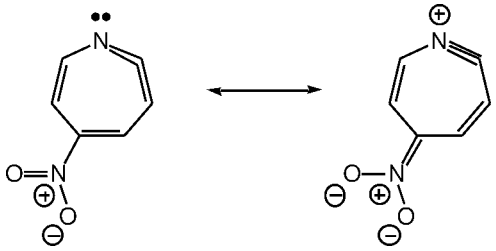

The greater contribution of the mesomer on the right with increased electron-withdrawing power is supported by the shortening of the C=N bond length in **5** with increasing Hammett σ (**5** *r*1 in Table II).

We note also that the difference in overall enthalpies of reaction influences the positions of the transition states in a manner consistent with the Hammond postulate [79]. Thus, the forming C—N bond in **2** is shortest for the endothermic case with the NHMe substituent (i.e., the TS structure is latest, **2** *r*3 in Table II), while the breaking C—C bond in **4** is shortest for the most exothermic nitro-substituted case (i.e., the TS structure is earliest, **4** *r*2 in Table II). The intermediate bicyclic benzazirine **3** must be regarded as somewhat remarkable, insofar as two of its bonds certainly must be among the weakest C—C and C—N bonds ever characterized—the bond strengths range from 0.4 to 8.7 kcal · mol^{-1} depending on the level of theory. The very weak C—C bond, to the extent it may be regarded as a 1,3-interaction in a didehydroazepine, is reminiscent of the situation found in *m*-benzynes [80–85] and corresponding pyridynes [84, 86]. As is found in these aryne systems, the shallow nature of the bond stretching coordinate gives rise to very large differences between the CAS and DFT levels of theory with respect to the C—C bond length in **3** (*r*2 in Table II).

Inspection of Figure 5 suggests that the separation in S1 and S3 state energies previously inferred to contribute to a higher ring-expansion barrier is indeed only present in the four cases where σ is more negative than −0.3 (although for *p*-OMe, an interestingly high S3 energy is predicted). Unfortunately, it is for exactly these kinds of substituents that it has not proven possible to measure accurate kinetic data for ring expansion because of rapid ISC rates. In the remaining sections, we examine more carefully the factors influencing the relative singlet state energies, and the degree to which ISC may be influenced by *para* substitution in the four systems for which we have characterized the ring expansion pathway.

ISODESMIC ANALYSIS

To further rationalize the mild substituent effect on the ring-expansion reaction coordinate, we consider the following isodesmic equation:

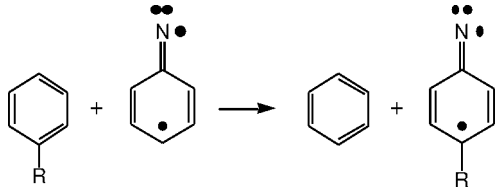

(1a)

for the S1 state. This reaction measures the additional resonance stabilization that is present when both the R group and the monovalent nitrogen are attached to the same aromatic ring, as opposed to being attached to distinct rings. For R = H, the change in enthalpy of the above reaction is zero by definition. For R = F and NO_2, this change in enthalpy at the CASPT2 level is calculated to be 0.5 kcal · mol^{-1} and 0.2 kcal · mol^{-1}, respectively, while at the DFT level it is precisely 0.0 kcal · mol^{-1} for both R groups. For R = NHMe, on the other hand, the change in enthalpy for Eq. (1a) is −4.0 kcal · mol^{-1} at the CASPT2 level and −5.5 kcal ·

mol^{-1} at the DFT level. Thus, the interaction between a strong donor group and the nitrene is stabilizing, but interaction between the nitrene and other groups either of lesser donating or of accepting character is negligible.

Thus, we conclude that the higher activation enthalpy for ring expansion in the *p*-NHMe-substituted case derives from a combination of reactant stabilization with this substituent, and product stabilization when the substituent is electron-withdrawing, as already discussed above. While we have not examined the reaction pathways for nitrenes substituted with other strong donating substituents, to the extent that the state energies for all cases with $\sigma < -0.3$ are similar, and that this situation is different from that found for all other substituents, we would expect such substituted nitrenes to exhibit activation enthalpies about as high as *p*-NHMe.

We examine the influence of substitution on state energies below, since there is some apparent correlation between the influence of substitution on this phenomenon and on the activation enthalpy for ring opening. Prior to doing so, however, it is appropriate to comment on the theoretically predicted activation enthalpies in comparison to those measured by Gritsan et al. [26, 38]. Based on a fairly complex kinetic analysis of different possible decomposition pathways for the singlet nitrene, these authors assigned Arrhenius activation energies of roughly 5.5 kcal · mol^{-1} for ring expansion of phenyl nitrene *para*-substituted with H, Me, CF_3, $CH_3C(O)$, and F. After subtracting *RT* to convert E_a to $\Delta H^{\ddagger}_{298}$, this value is within 4 kcal · mol^{-1} of the CASPT2 results for H and F (CASPT2 being the more reliable given the previously discussed instability of the DFT wave functions for TS structures **2**). We consider such a difference to be quite reasonable given the possible influence of solvation and the assumptions involved in the kinetic models. We note very recent work by Gritsan et al. on *p*-cyanophenylnitrene where E_a for ring expansion was measured as 7.2 ± 0.8 kcal · mol^{-1} and calculations at the CASPT2(8,8)/6-31G* level predicted 9.8 kcal · mol^{-1}, i.e., showing a very similar degree of difference [37].

Karney and Borden [14] have rationalized the overestimation of the ring-closure barrier heights at the CASPT2 level as deriving from a tendency for this method to overstabilize open-shell species (like the singlet) relative to closed-shell species (inferring the transition state to be closed-shell in nature). Our own experience with this methodological phenomenon, usually cited as having a magnitude of 3–5 kcal · mol^{-1} based on results for methylene reported by Andersson and Roos [52], is that (over a fairly wide variety of systems) it is much more variable, failing to be apparent in some systems [87] and being as large as 10 kcal · mol^{-1} in others [53]. Moreover, the instability of the restricted DFT SCF equations implies that **2** has a nontrivial degree of open-shell character, so any methodological imbalance should be reduced in magnitude. In the absence of demonstrating saturation with respect to basis set and active space size, and more firmly establishing the constants assumed in the kinetic analysis of the experimental data, we refrain from further interpreting theoretical/experimental disparities.

NITRENE STATE ENERGIES

To rationalize the observed energies of the various singlet states relative to T0, it is helpful to make use of the simplified two-electrons in two-orbitals configuration interaction model for diradicals of Michl and co-workers [41–43]. In this case, the two orbitals, denoted A and B as illustrated in Figure 7, are localized subject to the constraint that intraorbital electronic repulsion be maximal and interorbital repulsion minimal. For the nitrenes, the orbitals in question are in essence the in-plane nitrogen p orbital and the orbital π_4 of the phenylnitrene system (with substituents conjugating one or more p orbitals with the aromatic π system, the numbering of this orbital would change, and its shape would obviously be perturbed).

With these basis orbitals and neglecting normalization, the spatial parts of the triplet and three possible singlet states may be written as

$$T0 = |AB - BA\rangle \quad (2)$$

$$S1 = |AB + BA\rangle \quad (3)$$

$$S2 = |AA - BB\rangle \quad (4)$$

$$S3 = |AA + BB\rangle \quad (5)$$

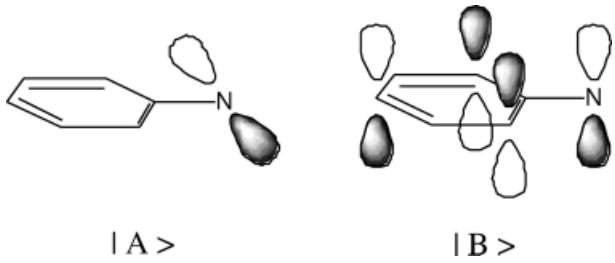

FIGURE 7. Localized orbitals A and B in (2,2) CI description.

If we define the energy of the triplet state as the relative zero, i.e.,

$$\langle \mathrm{T0}|H|\mathrm{T0}\rangle = 0 \tag{6}$$

where H is the Hamiltonian operator, then the energies of the singlet states can be determined from diagonalization of the 3×3 CI matrix

$$\mathbf{H} = \begin{bmatrix} 2K_{\mathrm{AB}} & 0 & \gamma \\ 0 & 2K_{\mathrm{ab}} & \delta \\ \gamma & \delta & 2(K_{\mathrm{AB}} + K_{\mathrm{ab}}) \end{bmatrix} \tag{7}$$

K_{ij} is a two-electron exchange integral defined in the usual way for spatial orbitals φ

$$K_{ij} = \iint \varphi_i^*(1)\varphi_i^*(2)\frac{1}{r_{12}}\varphi_j(1)\varphi_j(2)\, d\mathbf{r}(1)\, d\mathbf{r}(2) \tag{8}$$

where integration proceeds over the spatial coordinates of both electrons. Orbitals a and b are defined as the normalized linear combinations A + B and A − B, respectively. While there are some important caveats to using the same basis orbitals for every state in this analysis,* the simplicity of the formalism renders certain comparisons particularly clear that might otherwise be clouded, and in the interests of developing a qualitative understanding of the state-state interactions in the substituted nitrenes, we will proceed.

In a "perfect" biradical, there is no coupling between the states, and the CI matrix of Eq. (7) is diagonal, i.e., $\delta = \gamma = 0$. When A and B have nonzero overlap, the off-diagonal element γ quantifies the resonance between them. In the phenylnitrene case, there is no overlap, and $\gamma = 0$. Interaction between S2 and S3 derives from mixing of hole-pair configurations when there is some energy separation between orbitals A and B. Since orbitals A and B are not necessarily degenerate in the phenylnitrenes (although they may be accidentally so), δ is not required to be zero and its magnitude will affect the eigenvalues of **H**.

*Two of the most salient features of phenylnitrene are that the character of the lowest-energy singlet is open-shell and that the S–T splitting is only about half that found for the unsubstituted parent system, HN. Borden and co-workers have emphasized that these phenomena derive in large part from the ability of the phenyl group to delocalize the unpaired π electron in the singlet to create an iminyl/cyclohexadienyl-like biradical [3,11]. As the singlet state does not enjoy an exchange offset to Coulomb repulsion between the unpaired electrons, this is more stabilizing for the singlet than the triplet, and this rationalizes the reduction in splitting, but this also implies that orbital B for the singlet is really *different* than orbital B in the triplet, so that the simplified form of **H** in Eq. (7) is an idealization. Of course, this is true to a greater or lesser extent for *any* system where the biradical electrons interact.

Note that in the perfect biradical limit, the eigenvalue corresponding to the energy of S3 is equal to the sum of the eigenvalues for S1 and S2. At the CASPT2 level, for substituents having $-0.2 < \sigma < 0.9$, this is roughly the situation that obtains (vide infra for a discussion of DFT energies). Indeed, all singlet state energies for these species are successfully reproduced to within 2 kcal · mol^{-1} by taking $K_{\mathrm{AB}} = 9.5$, $K_{\mathrm{ab}} = 19$, and $\delta < 5$ (all units are kcal · mol^{-1}). In these nitrenes, then, to within 5 kcal · mol^{-1} there is an accidental near degeneracy between orbitals A and B. (The exact factor of 2 difference in K_{AB} and K_{ab} is coincidental.)

The insensitivity of δ to the presence of electron-withdrawing groups, which can in principle lower the energy of B relative to A by resonance, presumably owes to the highly electrophilic nature of nitrenes. The orbital energy separations between B and the lowest energy virtual (acceptor) orbitals of even the strongest electron-withdrawing groups are evidently too large for significant resonance.

That same low energy, however, permits the phenylnitrene B orbital to interact significantly with donor orbitals of sufficiently high energy. Such an interaction, as illustrated in Figure 8, will raise the energy of a hybrid B orbital while lowering the energy of the hybrid donor (usually lone-pair-like) orbital. If B begins below A in energy, in the absence of significant changes in the values of the exchange integrals, one would expect to initially see the S2–S3 energy separation reduce, reaching a minimum when $\delta = 0$, and then increase again as the hybrid B energy continues to be raised further above A. If, on the other hand, B begins higher in energy than A, there should be simply a steady increase in the S2–S3 energy separation as δ monotonically increases with increasingly negative values of σ. The latter situation corresponds best with the observed trends in CASPT2 energies, and hence we infer that B is slightly higher in energy than A for the unperturbed case, as illustrated in Figure 8. Given that a phenyl group is a donor substituent, this orbital energy ordering is to be expected if we consider phenylnitrene as a perturbation on imidogen (HN), where A and B are degenerate.

Note that the overall situation is quite different from that which is obtained for the formally isoelectronic phenylcarbenes [88, 89] and phenylnitrenium ions [67, 88]. In these latter species, there is a sizable separation between orbitals A and B (this can be immediately inferred on the basis of the lowest energy singlet states being closed-shell in nature, rather than open-shell), and thus one or the other of the

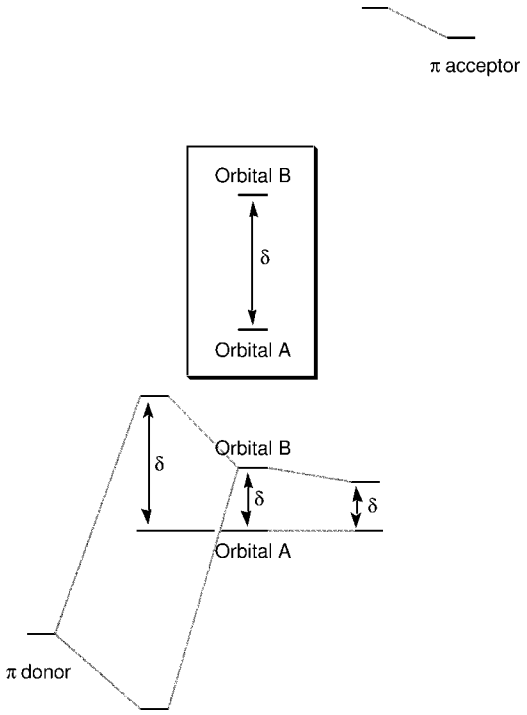

FIGURE 8. Mixing of the nitrene (2,2) CI orbitals with either a π donor (left) or a π acceptor (right). The difference in energy between orbitals A and (hybridized) B defines δ in Eq. (7). The inset indicates the higher orbital energies and greater interorbital separation that would be found were the orbitals to derive from a carbene instead of a nitrene.

two is well suited to mixing with either π-donors or π-acceptors, and as a result substitution effects on state-energy splittings are manifest over a broad range. The greater initial orbital splitting in the case of the carbene compared to the nitrene derives from the s character included in the in-plane orbital for the former but not the latter [15]; in the case of the nitrenium ion, this effect is further accentuated by the positive charge on the more electronegative nitrogen atom [88].

As to the question of whether the exchange integrals are indeed relatively constant with respect to substitution, it is trivial to investigate this question for the value of K_{AB}, since the CI matrix is block diagonal, and this exchange integral is the eigenvalue of its corresponding block of size 1. For all substituents except those having a σ value more negative than -0.14, the near constant T0–S1 energy separation (which is seen both at the CASPT2 and the BPW91 levels) implies a similarly constant value for the exchange integral. However, in the cases of the substituents having the most negative σ values, both levels of theory predict a decrease of about 2 kcal $\cdot$ mol^{-1} in the T0–S1 separation. This amounts, then, to a decrease of about 1 kcal $\cdot$ mol^{-1} in the exchange integral. Such a change is small enough that it may defy a definitive rationalization, but for the record we note that the direction of the change is in the direction expected. With increasing π-donor power, one expects the doubly occupied π orbitals to shift density in the direction of the nitrene nitrogen. To preserve orthogonality, the remaining π orbitals like orbital B must necessarily shift amplitude away from the nitrene nitrogen, and the greater spatial separation this induces between A (which must remain essentially entirely localized on the nitrene nitrogen) and B decreases the magnitude of the exchange integral. (We emphasize again that, within our analysis, the eigenvalue we are calling K_{AB} does derive from more than simply a difference in exchange, but the bottom line is that the net state-energy separation is largely insensitive to substitution effects.)

If we adopt a limiting value of 8 kcal $\cdot$ mol^{-1} for K_{AB} when the aromatic ring is substituted with a strong π donor, and maintain a value of 19 kcal $\cdot$ mol^{-1} for K_{ab}, the value of δ which best fits the CASPT2 data is 13 kcal $\cdot$ mol^{-1}. This increase in δ is consistent with the discussion above regarding resonance between B and the highest-energy conjugating orbital of the donor group.

DFT ENERGIES FOR THE SINGLET STATES

Application of the sum method to estimate S1 state energies provides values that are smaller than those predicted by CASPT2 (and smaller than experiment [5], in the case of PhN) by a fairly constant 4–5 kcal$\cdot$mol^{-1}. While the sum method is necessarily approximate, the assumptions behind its employment are perhaps more shaky in their application here than would otherwise be typical. The derivation of Eq. (1) requires that the spatial components of all corresponding singlet and triplet orbitals be identical; however, as already emphasized [88], that is by no means a good assumption for the biradical orbitals in T0 and S1. Nevertheless, the DFT energies do show the same trend as the CASPT2 energies for this state as a function of subsitution. Thus, the DFT results bolster the qualitative aspects of our analysis here even though they provide less useful quantiative information.

On the other hand, BPW91 predicts a much greater sensitivity of states S2 and S3 to substitution than does the CASPT2 level of theory. For

state S2, the fairly consistent difference of about 2–5 kcal · mol^{-1} between the BPW91 and CASPT2 results is probably attributable to the CASPT2 tendency to overestimate triplet stabilities relative to closed-shell singlets, and thus the DFT numbers are likely to be more reliable. DFT results for the triplet-closed-shell-singlet splittings in the isoelectronic systems phenylcarbene and phenylnitrenium ion further support this contention [88–93]. For S3, on the other hand, the much larger difference between the two levels of theory, the nature of the state as a metastable minimum in the SCF coefficient space, and the failure of fundamental theory to provide a formal justification for application to such an excited state, all suggest that the DFT numbers should be viewed with suspicion.

Furthermore, within the (2,2) CI approach, the only way in which S2 and S3 can become degenerate, as they approximately are at the BPW91 level for substituents having very high positive σ values, is for K_{AB} to be zero. However, if this is the case, then inspection of Eq. (7) (recalling that $\gamma = 0$ by symmetry) makes it clear that the triplet and the open-shell singlet must also be degenerate, which is contrary to what is predicted by both levels of theory. Thus, in spite of the likely quality of the DFT values for the energy of S2, we must conclude that the S3 energies are untrustworthy and should not be interpreted.

SPIN-ORBIT COUPLING

Miura and Kobayashi [94] and Gritsan et al. [26] have observed the rates of ISC in phenylnitrenes to increase substantially when strong donor groups are present—a rough estimate is a factor of 1000 for a strong π donor compared to the parent system. For biradicals where the two electrons are spatially proximate, as in nitrenes, SOC is the primary mechanism for ISC. For small values of SOC, relative rates k_{ISC} between two systems can be estimated from the Landau–Zener model as [42]

$$\frac{k'_{ISC}}{k_{ISC}} = \left(\frac{\langle S1|H_{SO}|T0\rangle'}{\langle S1|H_{SO}|T0\rangle}\right)^2 \left(\frac{\Delta E}{\Delta E'}\right)^2 \qquad (9)$$

where H_{SO} is the spin-orbit coupling Hamiltonian, and ΔE is the energy difference between state T0 and S1. In the phenylnitrenes, however, the SOC matrix elements between T0 and S1 are required by symmetry to be zero. Thus, SOC can only be accomplished by dynamical means, whereby S2 and/or S3 character can be mixed into S1 by geometric distortion.

The second term on the right-hand side of Eq. (9)—the square of the ratio of the T0–S1 splittings—cannot account for a change in ISC of more than about 1.4 based on the data in Table III for donor-substituted systems compared to the parent. Thus, to rationalize the large increases in ISC observed by Gritsan et al., we must look to the SOC matrix elements.

To obtain a qualitative picture of SOC in the nitrenes, we again turn to the (2,2) CI model. For the electrons in the active space of this model, the two-electron contribution to SOC is negligible [43]. The two-electron contribution between the active electrons and the frozen core may be significant, but typically it is opposite in sign and only one half of the magnitude of the one-electron contributions. For the nonmixing wave functions of a perfect biradical, one-electron SOC matrix elements are nonzero only between S3 and T0. For any other singlet to exhibit nonzero SOC, it must develop some S3 character via mixing of states. Thus, for instance, the SOC constants for the S2 states of **1** become larger with the strength of the donor group due to the already discussed increase in δ which increases the mixing of S2 and S3 [Eq. (7), Table IV, and Fig. 8]. The magnitude of SOC depends linearly on the coefficient of S3 in the mixed singlet. We can determine this coefficient from diagonalizing the CI matrix of Eq. (7). Using the appropriate values discussed above for the exchange integrals and off-diagonal matrix elements δ, we predict the contribution of the diabatic S3 state (i.e., pre-diagonalization) to the adiabatic S2 state (i.e., postdiagonalization) to be about three times larger for R = NHMe than for R = NO_2. This is about double the factor derived from explicit calculation of SOC (Table IV), reflecting the qualitative nature of the (2,2) CI model.

For SOC to be nonzero for S1, some distortion must occur to transfer S3 character into S1. One of the softest modes of distortion in **1** is along the reaction coordinate connecting for ring expansion already discussed above. Distortion along this mode allows bonding to occur between localized orbitals A and B, and thus results in nonzero values of γ, the matrix element that specifically mixes S3 and S1. Moreover, since δ is also nonzero, all three singlets mix either directly or indirectly, as anticipated from the loss of all symmetry elements in TS structure **2**.

If we assume only a small mixing of S1 and S3, by choosing $\gamma < 5$ kcal · mol^{-1}, and use the values discussed above for the exchange integrals and δ for the case of R = NHMe versus R = H, then the

ratio of the S3 coefficients in the S1 expansions is roughly 3 for these two substitutents. Squaring this, and multiplying by a factor of 1.4 from the difference in the T0–S1 energy separations, we predict about a 15-fold increase in the ISC rate for the system substituted with a strong electron donor. This prediction is about 2 orders of magnitude smaller than what is observed experimentally [26], and the discrepancy most likely derives from our choice of γ, which is entirely arbitrary, and from the assumption that the values of the exchange integrals and δ are constant and unaffected by dynamic behavior. However, the vibrationally averaged SOC matrix elements required for a more quantitative evaluation are beyond the scope of the present work, and we will not proceed here beyond our qualitative rationalization of the observed *trend* in ISC rate constants.

IMPLICATIONS FOR PHOTOAFFINITY LABELS

These and earlier [12] results, taken together with the seminal work of Karney and Borden [14], suggest that both electronic and steric effects can influence the proclivity of an arylnitrene to ring-expansion. However, while steric effects will obviously be manifest for *any ortho* substituent, in proportion to its size, electronic effects appear to become important only after a certain threshold of donating power has been reached, owing to the orbital energy situation that is obtained in the phenylnitrene system. To the extent that strong donors also appear to increase rates of undesirable ISC, engineering of steric factors seems more profitable in future molecular design. Indeed, there may be an opportunity to take advantage of a certain synergy in this regard. Bulky *ortho* groups should serve not merely to decrease rates of ring expansion, but also to decrease fluxionality in the system as a whole. In that case, dynamical mixing of S1 and S3 may well be decreased, and strong donors at the *para* position should then be able to play a favorable role in *further* increasing the activation enthalpy for ring expansion without playing a negative role by contributing to higher rates of ISC. Such predictions will hopefully prove useful for the design of future experiments.

ACKNOWLEDGMENTS

We are grateful for financial support from the National Science Foundation, and for high-performance computing resources made available by the Minnesota Supercomputer Institute. This work was also supported in part by the Alfred P. Sloan and John Simon Guggenheim Foundations, the Spanish Ministry of Education and Culture, and Fundación BBV. We thank W. T. Borden and M. S. Platz for comments filled with (the usual) penetrating insights.

References

1. Gilchrist, T. L.; Rees, C. W. Carbenes, Nitrenes, and Arynes; Nelson London, 1969.
2. Platz, M. S. Acc Chem Res 1995, 28, 487.
3. Borden, W. T.; Gritsan, N. P.; Hadad, C. M.; Karney, W. L.; Kemnitz, C. R.; Platz, M. S. Acc Chem Res 2000, 33, 765.
4. Schuster, G. B.; Platz, M. S. Adv Photochem 1992, 17, 69.
5. Travers, M. J.; Cowles, D. C.; Clifford, E. P.; Ellison, G. B. J Am Chem Soc 1992, 114, 8699.
6. McDonald, R. N.; Davidson, S. J. J Am Chem Soc 1993, 115, 10857.
7. Gritsan, N. P.; Yuzawa, T.; Platz, M. S. J Am Chem Soc 1997, 119, 5059.
8. Kozankiewicz, B.; Deperasińska, I.; Zhai, H. B.; Zhu, Z.; Hadad, C. M. J Phys Chem A 1999, 103, 5003.
9. Gritsan, N. P.; Zhu, Z.; Hadad, C. M.; Platz, M. S. J Am Chem Soc 1999, 121, 1202.
10. Kim, S.-J.; Hamilton, T. P.; Schaefer, H. F., III. J Am Chem Soc 1992, 114, 5349.
11. Hrovat, D. A.; Waali, E. E.; Borden, W. T. J Am Chem Soc 1992, 114, 8698.
12. Smith, B. A.; Cramer, C. J. J Am Chem Soc 1996, 118, 5490.
13. Castell, O.; Garcia, V. M.; Bo, C.; Caballol, R. J Comput Chem 1996, 17, 42.
14. Karney, W. L.; Borden, W. T. J Am Chem Soc 1997, 119, 3347.
15. Kemnitz, C. R.; Karney, W. L.; Borden, W. T. J Am Chem Soc 1998, 120, 3499.
16. Banks, R. E.; Prakash, A. Tetrahedron Lett 1973, 2, 99.
17. Banks, R. E.; Prakash, A. J Chem Soc Perkin Trans 1974, 1, 11365.
18. Poe, R.; Schnapp, K.; Young, M. J. T.; Grayzar, J.; Platz, M. S. J Am Chem Soc 1992, 114, 5054.
19. Cai, S. X.; Glenn, D. J.; Keana, J. F. W. J Org Chem 1992, 57, 1299.
20. Schnapp, K. A.; Platz, M. S. Bioconjugate Chem 1993, 4, 178.
21. Schnapp, K. A.; Poe, R.; Leyva, E.; Soundararajan, N.; Platz, M. S. Bioconjugate Chem 1993, 4, 172.
22. Zhai, H.; Platz, M. S. J Phys Org Chem 1997, 10, 22.
23. Pandurangi, R. S.; Karra, S. R.; Kuntz, R. R.; Volkert, W. A. Photochem Photobiol 1997, 65, 208.
24. Pandurangi, R. S.; Karra, S. R.; Katti, K. V.; Kuntz, R. R.; Volkert, W. A. J Org Chem 1997, 62, 2798.
25. Gritsan, N. P.; Zhai, H. B.; Yuzawa, T.; Karweik, D.; Brooke, J.; Platz, M. S. J Phys Chem A 1997, 101, 2833.
26. Gritsan, N. P.; Tigelaar, D.; Platz, M. S. J Phys Chem A 1999, 103, 4465.

27. Gritsan, N. P.; Gudmundsdóttir, A. D.; Tigelaar, D.; Platz, M. S. J Phys Chem A 1999, 103, 3458.
28. Pol'shakov, D. A.; Tsentalovich, Y. P.; Gritsan, N. P. Russ Chem Bull 2000, 49, 50.
29. McClelland, R. A.; Davidse, P. A.; Hadzialic, G. J Am Chem Soc 1995, 117, 4173.
30. McClelland, R. A.; Kahley, M. J.; Davidse, P. A. J Phys Org Chem 1996, 9, 355.
31. McLelland, R. A.; Gadosy, T. A.; Ren, D. Can J Chem 1998, 76, 1327.
32. Ramlall, P.; Li, Y. Z.; McClelland, R. A. J Chem Soc Perkin Trans 1999, 2, 1601.
33. Bose, R.; Ahmad, A. R.; Dicks, A. P.; Novak, M.; Kayser, K. J.; McClelland, R. A. J Chem Soc Perkin Trans 1999, 2, 1591.
34. Gadosy, T. A.; McClelland, R. A. J Am Chem Soc 1999, 121, 1459.
35. March, J. Advanced Organic Chemistry, 4th ed.; Wiley: New York, 1992.
36. Karney, W. L.; Borden, W. T. J Am Chem Soc 1997, 119, 1378.
37. Gritsan, N. P.; Likhotvorik, I.; Tsao, M.-L.; Çelebi, N.; Platz, M. S.; Karney, W. L.; Kemnitz, C. R.; Borden, W. T. J Am Chem Soc 2001, 123, 1425.
38. Gritsan, N. P.; Gudmundsdóttir, A. D.; Tigelaar, D.; Zhu, Z.; Karney, W. L.; Hadad, C. M.; Platz, M. S. J Am Chem Soc 2001, 123, 1951.
39. Hammett, L. P. Chem Rev 1935, 17, 125.
40. Correlation Analysis in Chemistry: Recent Advances; Chapman, N. B.; Shorter, J., Eds.; Plenum: New York, 1978.
41. Bonacic-Koutecky, V.; Koutecky, J.; Michl, J. Angew Chem Int Ed Engl 1987, 26, 170.
42. Michl, J.; Bonacic-Koutecky, V. Electronic Aspects of Organic Photochemistry; Wiley: New York, 1990; p. 367.
43. Michl, J. J Am Chem Soc 1996, 118, 2568.
44. Roos, B. O. In Ab Initio Methods in Quantum Chemistry; Lawley, K. P., Ed.; Wiley: New York, 1987; Vol. 2, p. 399.
45. Dunning, T. H. J Chem Phys 1989, 90, 1007.
46. Barandiaran, Z.; Seijo, L. Can J Chem 1992, 70, 409.
47. Barandiaran, Z.; Seijo, L. J Chem Phys 1994, 101, 4049.
48. Hehre, W. J.; Radom, L.; Schleyer, P. v. R.; Pople, J. A. Ab Initio Molecular Orbital Theory; Wiley: New York, 1986.
49. Schmidt, M. W.; Gordon, M. S. Annu Rev Phys Chem 1998, 49, 233.
50. Andersson, K.; Malmqvist, P.-Å.; Roos, B. O.; Sadlej, A. J.; Wolinski, K. J Phys Chem 1990, 94, 5483.
51. Andersson, K.; Malmqvist, P.-Å.; Roos, B. O. J Chem Phys 1992, 96, 1218.
52. Andersson, K.; Roos, B. O. Int J Quantum Chem 1993, 45, 591.
53. Lim, M. H.; Worthington, S. E.; Dulles, F. J.; Cramer, C. J. In Density-Functional Methods in Chemistry; Laird, B. B.; Ross, R. B.; Ziegler, T., Eds.; American Chemical Society: Washington, DC, 1996; Vol. 629, p. 402.
54. Andersson, K.; Blonberg, M. R. A.; Fülscher, M. P.; Karlström, G.; Lindh, R.; Malmqvist, P.-Å.; Neogrády, P.; Olsen, J.; Roos, B. O.; Sadlej, A. J.; Schütz, M.; Seijo, L.; Serrano-Andrés, L.; Siegbahn, P. E. M.; Widmark, P.-O. MOLCAS-4; Lund, Sweden, 1997.
55. Frisch, M. J.; Trucks, G. W.; Schlegel, H. B.; Gill, P. M. W.; Johnson, B. G.; Robb, M. A.; Cheeseman, J. R.; Keith, T. A.; Petersson, G. A.; Montgomery, J. A.; Raghavachari, K.; Al-Laham, M. A.; Zakrzewski, V. G.; Ortiz, J. V.; Foresman, J. B.; Peng, C. Y.; Ayala, P. A.; Wong, M. W.; Andres, J. L.; Replogle, E. S.; Gomperts, R.; Martin, R. L.; Fox, D. J.; Binkley, J. S.; Defrees, D. J.; Baker, J.; Stewart, J. P.; Head-Gordon, M.; Gonzalez, C.; Pople, J. A. Gaussian 98; Gaussian, Inc.: Pittsburgh, PA, 1998.
56. Werner, H.-J.; Knowles, P. J.; Amos, R. D.; Lindh, R.; Lloyd, A. W.; McNicholas, S. J.; Manby, F. R.; Meyer, W.; Mura, M. E.; Nicklass, A.; Palmieri, P.; Pitzer, R.; Rauhut, G.; Schütz, M.; Stoll, H.; Stone, A. J.; Tarroni, R.; Thorsteinsson, T. MOLPRO 2000; Stuttgart, Germany.
57. Schmidt, M. W.; Baldridge, K. K.; Boatz, J. A.; Elbert, S. T.; Gordon, M. S.; Jensen, J. H.; Koseki, S.; Matsunaga, N.; Nguyen, K. A.; Su, S.; Windus, T. L.; Dupuis, M.; Montgomery, J. A. J Comput Chem 1993, 14, 1347.
58. Becke, A. D. Phys Rev A 1988, 38, 3098.
59. Perdew, J.; Wang, Y. Phys Rev B 1992, 45, 13244.
60. Lee, C.; Yang, W.; Parr, R. G. Phys Rev B 1988, 37, 785.
61. Hay, P. J.; Wadt, W. R. J Chem Phys 1985, 82, 270.
62. Hay, P. J.; Wadt, W. R. J Chem Phys 1985, 82, 284.
63. Hay, P. J.; Wadt, W. R. J Chem Phys 1985, 82, 299.
64. Hohenberg, P.; Kohn, W. Phys Rev B 1964, 3, 864.
65. Gunnarsson, O.; Lundqvist, B. I. Phys Rev B 1976, 13, 4274; Erratum 1976, 15, 6006.
66. Worthington, S. E.; Cramer, C. J. J Phys Org Chem 1997, 10, 755.
67. Sullivan, M. B.; Brown, K.; Cramer, C. J.; Truhlar, D. G. J Am Chem Soc 1998, 120, 11778.
68. Cramer, C. J.; Thompson, J. J Phys Chem A 2001, 105, 2091.
69. Cai, Z. L.; Tozer, D. J.; Reimers, J. R. J Chem Phys 2000, 113, 7084.
70. Ziegler, T.; Rauk, A.; Baerends, E. J. Theor Chim Acta 1977, 43, 261.
71. Noodleman, L.; Post, D.; Baerends, E. J. Chem Phys 1982, 64, 159.
72. Cramer, C. J.; Dulles, F. J.; Giesen, D. J.; Almlöf, J. Chem Phys Lett 1995, 245, 165.
73. Davidson, E. Int J Quantum Chem 1998, 69, 241.
74. Gräfenstein, J.; Kraka, E.; Cremer, D. Chem Phys Lett 1998, 288, 593.
75. Gräfenstein, J.; Cremer, D. Phys Chem Chem Phys 2000, 2, 2091.
76. Gräfenstein, J.; Hjerpe, A. M.; Kraka, E.; Cremer, D. J Phys Chem A 2000, 104, 1748.
77. de Visser, S. P.; Filatov, M.; Shaik, S. Phys Chem Chem Phys 2000, 2, 5046.
78. Ellison, G. B. personal communication of unpublished results.
79. Hammond, G. S. J Am Chem Soc 1955, 77, 334.
80. Kraka, E.; Cremer, D. J Am Chem Soc 1994, 116, 4929.
81. Kraka, E.; Cremer, D.; Bucher, G.; Wandel, H.; Sander, W. Chem Phys Lett 1997, 268, 313.
82. Cramer, C. J.; Nash, J. J.; Squires, R. R. Chem Phys Lett 1997, 277, 311.

83. Sander, W. Acc Chem Res 1999, 32, 669.
84. Debbert, S. L.; Cramer, C. J. Int J Mass Spectrom 2000, 201, 1.
85. Johnson, W. T. G.; Cramer, C. J. J Am Chem Soc 2001, 123, 923.
86. Cramer, C. J.; Debbert, S. Chem Phys Lett 1998, 287, 320.
87. Cramer, C. J. J Chem Soc Perkin Trans 1999, 2, 2273.
88. Cramer, C. J.; Dulles, F. J.; Falvey, D. E. J Am Chem Soc 1994, 116, 9787.
89. Geise, C. M.; Hadad, C. M. J Org Chem 2000, 65, 8348.
90. Wong, M. W.; Wentrup, C. J Org Chem 1996, 61, 7022.
91. Schreiner, P. R.; Karney, W. L.; Schleyer, P. v. R.; Borden, W. T.; Hamilton, T. P.; Schaefer, H. F., III. J Org Chem 1996, 61, 7030.
92. Patterson, E. V.; McMahon, R. J. J Org Chem 1997, 62, 4398.
93. Cramer, C. J.; Falvey, D. E. Tetrahedron Lett 1997, 38, 1515.
94. Miura, A.; Kobayashi, T. J Photochem Photobiol A Chem 1990, 53, 223.